Available online at www.sciencedirect.com
ScienceDirect
Trans. Nonferrous Met. Soc. China 21(2011) 1225−1233
Transactions of Nonferrous Metals Society of China
www.tnmsc.cn

Fatigue fracture mechanism of AZ31B magnesium alloy and its welded joint

ZHANG Hong-xia, WANG Wen-xian, WEI Ying-hui, LI Jin-yong, WANG Jian-ling

College of Materials Science and Engineering, Taiyuan University of Technology, Taiyuan 030024, China

Received 16 July 2010; accepted 20 November 2010

Abstract: Fatigue test was carried out on AZ31B magnesium alloy. Under 2×10^6 cycle times, the fatigue strengths of base metal (BM), butt joint (BJ), transverse cross joint (TJ), lateral connection joint (LJ) are 66.72, 39.00, 24.38 and 24.40 MPa, respectively. The crack propagation behavior of the alloy was analyzed by optical microscopy. The AZ31B magnesium alloy base metal has a smooth crack propagation macroscopic path. However, the microscopic path is twisted and some cracks have two forks, and the crack propagation is transgranular. The crack initiates in the weld toe and the crack propagates along the HAZ for the BJ and TJ; for the LJ crack initiates in the fillet weld leg. The fatigue fracture mechanisms were analyzed by SEM. The fatigue fracture surface consists of quasi-cleavage patterns or cleavage step and a brittle fracture occurs. Numerous secondary cracks are observed; some fatigue striations exist in butt joint and its size is about 5 μm.

Key words: AZ31B magnesium alloy; fatigue fracture; crack propagation; brittle fracture

1 Introduction

Magnesium alloys have excellent mechanical properties such as high specific strength at room temperature and superplasticity at elevated temperatures [1−2]. Magnesium alloys are increasingly considered the advanced materials that comply with energy conservation and environmental pollution regulations [3]. They are also hailed as the most developmental potential among all alloys and are prospective green engineering structure materials of the 21st century [4−5].

Fatigue fracture is a major failure pattern in metal structures, and 70% to 90% of failure accidents involving welded structures are caused by the fatigue fracture of welded joints. Welded structures are used in most buildings and construction projects, and the accidents stemming from fatigue damage often result in a catastrophic loss of lives and property. The weldability [6], welding technology adaptability, microstructure [7] and mechanical properties [8−9] of magnesium alloys were widely studied. However, only a few studies focused on the fatigue properties of magnesium alloy welded joints [10−11]. These researchers mainly studied the tensile properties and the influence of welding processes on fatigue properties of magnesium alloy. The research about fatigue fracture mechanism of welded joint is less. Investigations on the fatigue properties of magnesium alloy welded joints under dynamic loading have theoretical and practical significance in engineering applications.

Wrought magnesium alloys have higher mechanical properties, including tensile strength and elongation, as well as higher corrosion resistance and fatigue properties compared with cast magnesium alloys [12−13]. These characteristics make wrought magnesium alloys suitable for a wide range of applications. In this investigation, the rolled AZ31B magnesium alloy and its welded joint are tested for fatigue property, and their crack propagation feature and fatigue fracture mechanism are analyzed.

2 Experimental

2.1 Materials

A 10 mm-thick rolled AZ31B magnesium alloy plate was used in the experiment, and its chemical composition is listed in Table 1.

2.2 Welding methods and welding technology

Manual TIG welding method and a 300 GP AC/DC TIG welding equipment were used to weld the AZ31B magnesium alloy with an AZ31B magnesium alloy

Foundation item: Project (50675148) supported by the National Natural Science Foundation of China
Corresponding author: WANG Wen-xian; Tel: +86-351-6010076; E-mail: wwx960@126.com
DOI: 10.1016/S1003-6326(11)60846-7

welding wire (*d* 2.8 mm). The parameters of the welding process are listed in Table 2.

Table 1 Chemical composition of AZ31B (mass fraction, %)

Al	Zn	Mn	Ca	Si
2.5−3.5	0.6−1.4	0.2−1.0	0.04	0.10
Cu	Ni	Fe	Mg	
0.01	0.001	0.005	Bal.	

Table 2 Welding process parameters

Joint type	Welding current/A	Welding voltage/V	Welding speed v/(mm·s^{-1})
Butt joint	170−180	12–15	2.8–3.0
Transverse cross joint	170−180	12–15	2.5–2.9
Lateral connection joint	160−170	12–15	2.4–2.9

2.3 Specimen processing

The AZ31B magnesium alloy base metal was mechanically processed. The welded joint was first welded and then processed. The size and shape of the fatigue specimens are given in Fig. 1.

3 Results and discussion

3.1 Metallograph analysis

The microstructure of cross section of AZ31B magnesium alloy was analyzed. The microstructure (Fig. 2) indicates that the grain size is nonuniform, and some precipitated phases are observed inside grains and at grain boundaries.

The microstructures of the welded joint of the alloy are shown in Fig. 3. Figure 3(a) shows the microstructure of the welding center region, where the grain size is uniform and has a typical isometric feature.

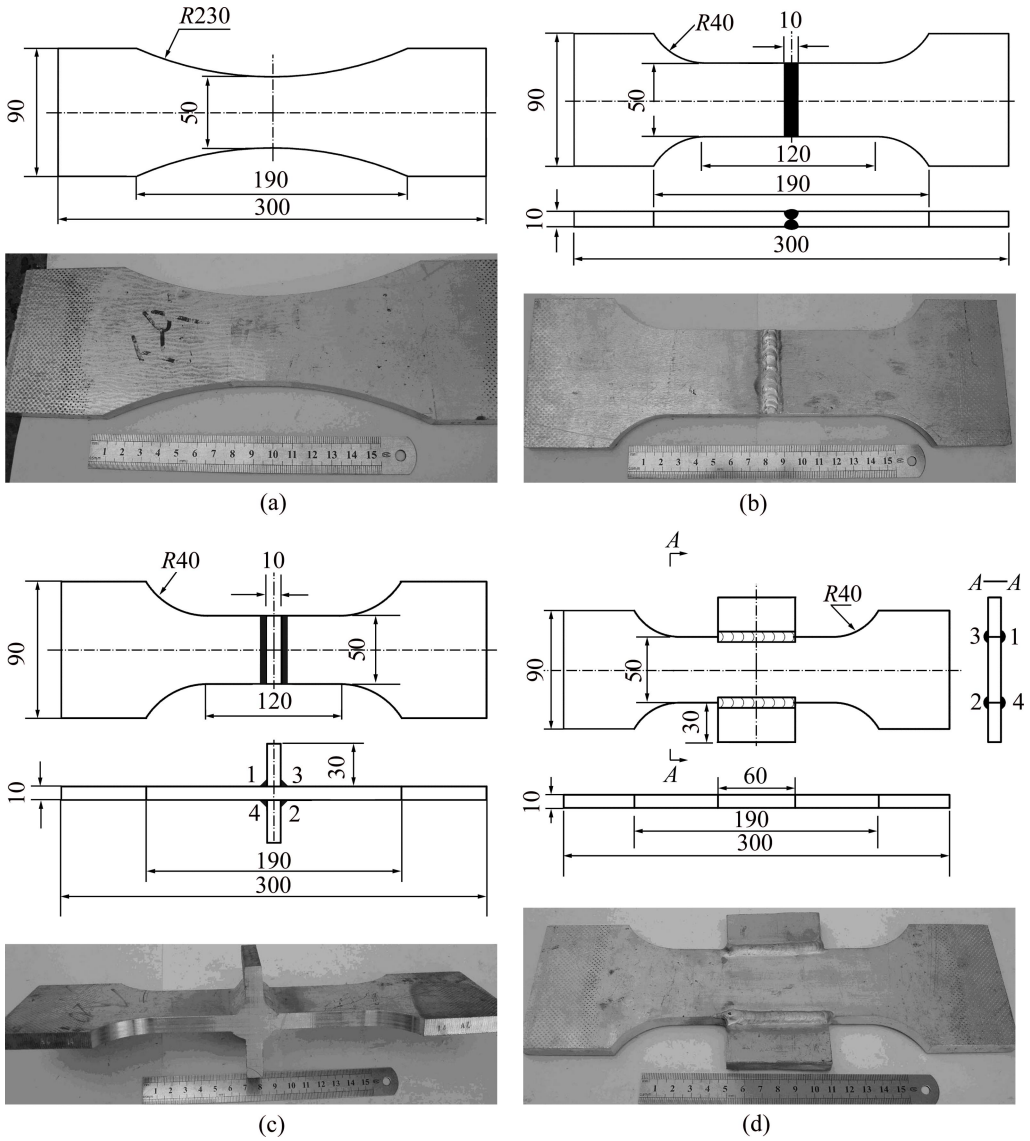

Fig. 1 Size and shape of AZ31B magnesium alloy fatigue specimens: (a) Base metal; (b) Butt joint; (c) Transverse cross joint; (d) Lateral connection joint (unit: mm)

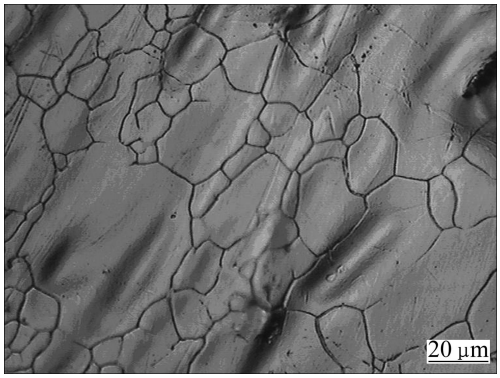

Fig. 2 Microstructure of AZ31 magnesium alloy

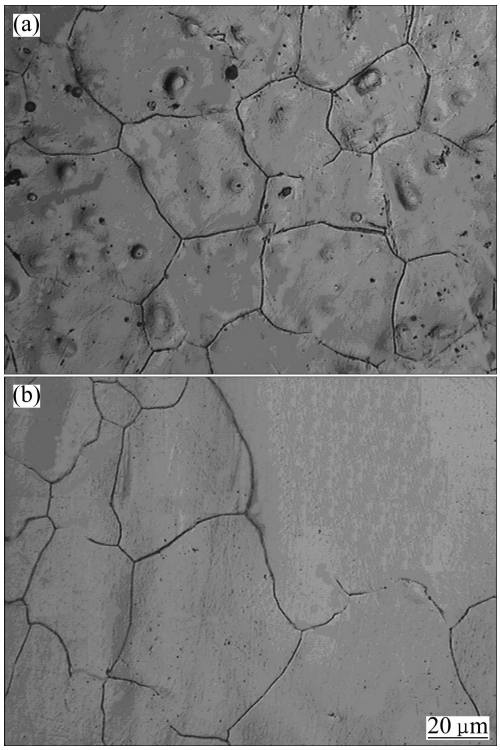

Fig. 3 Microstructures of welded joint: (a) Welding center; (b) HAZ

An intragranular precipitate phase is present. Figure 3(b) shows the microstructure of the HAZ region, where the grains are coarse and nonuniform.

3.2 Fatigue test

Fatigue tests were conducted using a PLG−200D high frequency fatigue testing machine with a stress ratio of zero. The imposed cyclic frequency varies between 99−102 Hz.

3.2.1 Fatigue test results

AZ31B magnesium alloy and its welded joint were tested. The fatigue test results are listed in Table 3. It can be noted that specimens 1 to 6 for the base metal are all disabled in the middle of gage length, and the specimens 7 and 8 are unfaulted under 5×10^6 cycles. Furthermore, specimens 1 to 7 for the welded joint are all disabled in the welding toe, and specimen 8 is unfaulted under 5×10^6 cycles.

Using the fatigue results given in Table 3, the nominal stress S—N curves of the AZ31B magnesium alloy base metal and welded joint are depicted in Fig. 4. Every group test data are divided into two parts by the curves in Fig. 4. The upper part is the fatigue fracture zone and the bottom is the no-fatigue fracture zone.

Table 4 shows that the fatigue strengths corresponding to a 50% survival rate for the base metal, butt joint, transverse cross joint, and lateral connection joint are 66.72, 39.00, 24.38, and 24.40 MPa, respectively. The fatigue property of the welded joint is lower than that of the base metal. The fatigue properties of the butt joint, transverse cross joint and lateral connection joint are 58.4%, 36.5%, and 36.6% of that of base metal, respectively. This is due to the stress concentration and welding residual stress in the welded joint. The coefficient of stress concentration is different in three joint and the dynamic load carrying capacity of welded structure is closely related to the joint type.

Table 3 Fatigue test results of AZ31B

Specimen	Nominal stress range, $\Delta\sigma_{nom}$/MPa				Number of cycles to failure, $N/10^6$				Disabled position	
	Base metal	Butt joint	Transverse cross joint	Lateral connection joint	Base metal	Butt joint	Transverse cross joint	Lateral connection joint	Base metal	Joint
1	100	60	50	70	0.231	0.266	0.298	0.103	In gage length	Weld toe
2	90	55	40	60	0.385	0.460	0.329	0.204	In gage length	Weld toe
3	85	50	45	40	0.406	0.580	0.403	0.218	In gage length	Weld toe
4	80	50	30	30	0.402	0.446	0.846	1.308	In gage length	Weld toe
5	75	45	35	25	0.497	1.320	0.298	2.332	In gage length	Weld toe
6	70	40	35	35	2.524	2.442	0.426	0.971	In gage length	Weld toe
7	65	35	25	20	5.000	3.215	1.919	2.566	Unfaulted	Weld toe
8	55	30	20	15	5.000	5.011	5.041	5.000	Unfaulted	Unfaulted

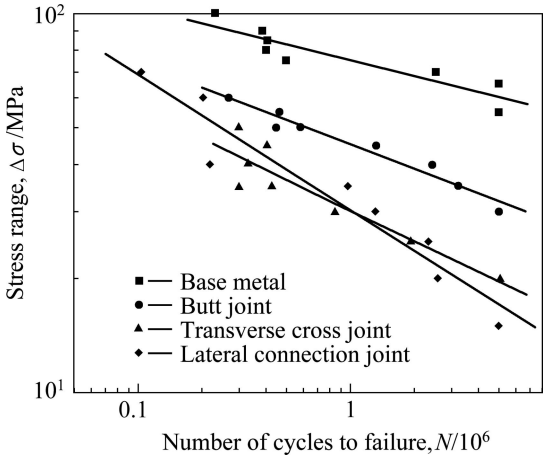

Fig. 4 *S*—*N* curves of magnesium alloy AZ31B and welded joints

Table 4 *S*—*N* curve parameters of AZ31B and welded joints

Joint type	*m*		C_m	$\Delta\sigma_m$/MPa	*r*
	Result	Deviation			
Base metal	6.87	0.026	6.76×10^{18}	66.72	0.901
Butt joint	4.70	0.033	5.99×10^{13}	39.00	0.895
Transverse cross joint	3.58	0.019	1.84×10^{11}	24.38	0.958
Lateral connection joint	2.72	0.046	1.58×10^{10}	24.40	0.949

The parameters can fit formula $N(\Delta\sigma)^m=C_m$ in Table 4, *m* and c_m are material constants, the correlation coefficients (*r*) of *S*—*N* curves are nearly greater than 0.9 and the deviations of *m* are lower, which indicate that the tested data are reliable.

3.2.2 Fatigue crack propagation path

The fatigue failure site and crack propagation macrographs of magnesium alloy and its welded joint are shown in Fig. 5.

The crack initiation site for the base metal locates at the smallest section as shown in Fig. 5(a), and the crack propagation direction is vertical to the load direction. The crack initiation site for the welded joint is at the welding toe, as shown in Fig. 5(b), the butt joint crack propagates along the HAZ in the welding direction and cross section due to the coarse microstructure. For the transverse cross joint, the crack initiates at the welding toe, and propagates along the weld junction in the welding direction and vertical to the load direction; it propagates along the HAZ in the cross section as shown in Fig. 5(c). Figure 5(d) shows the crack initiation site for the lateral connection joint. The crack initiation site is in fillet weld leg, and the direction of crack propagation is vertical to the load direction. Since the stress concentration is greater in welding toe and fillet weld leg, the crack initiation occurs at these sites.

A CMM−20 optical microscope was used to determine the fatigue crack propagation behavior. The fatigue crack propagation path for the AZ31B magnesium alloy base metal is shown in Fig. 6. The macroscopic path of the crack propagation of AZ31 magnesium alloy base metal is smooth (Fig. 5(a)). However, the microscopic path is twisted. Some cracks

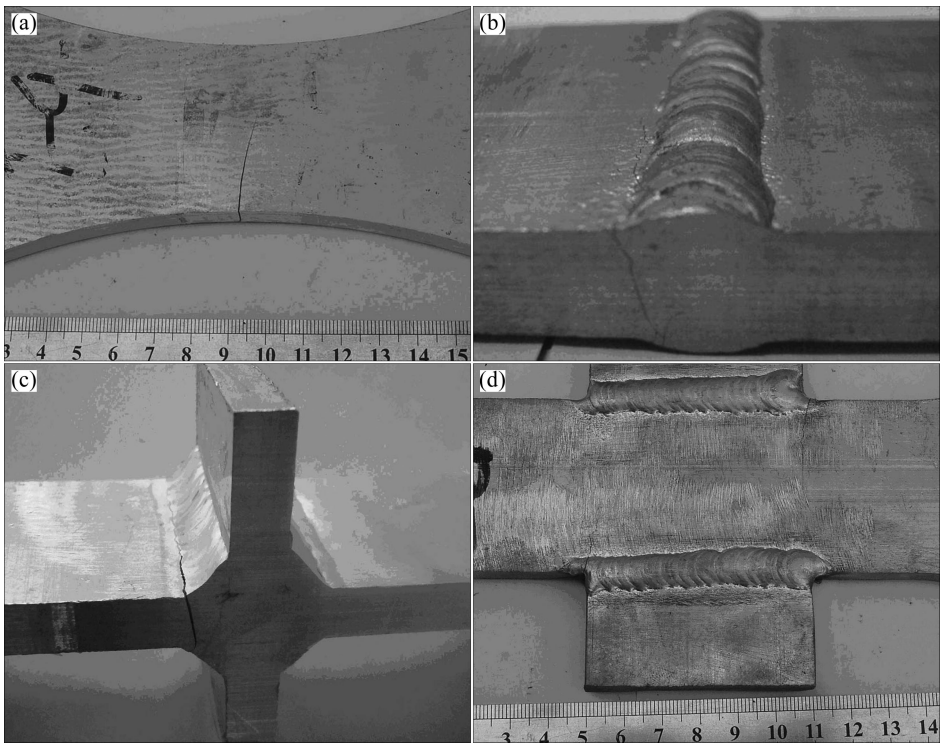

Fig. 5 Fatigue crack initiation, propagation site and direction: (a) Base metal; (b) Butt joint; (c) Transverse cross joint; (d) Lateral connection joint

also have two forks.

Figure 7 shows the crack propagation photographs of the base metal. The crack propagation is transgranular as shown in Figs. 7(a) and (b). The transgranular fracture plays a predominant role in the fatigue crack propagation track and it is a brittle fracture. Figure 7(c) shows the crack tip propagation. Slip deformation can be seen from the base metal with some precipitated phases. Deformation bands near the crack are observed in Fig. 7(d), and twins are present in the course of crack propagation. It can be found that crack propagation deformation also depends on twins because the slip system is less at room temperature.

The crack of the butt joint initiates at the weld toe along the weld direction (Fig. 8). Figures 8(a) and (b) show crack tip initiation sites of the weld cross section. Figure 8(b) shows the crack propagation along the HAZ. Figures 8(c) and (d) show photographs of the crack propagation along the weld direction, where the crack propagates along the weld junction. Figure 8(d) indicates that the AZ31 magnesium alloy butt joint exhibits a brittle fracture.

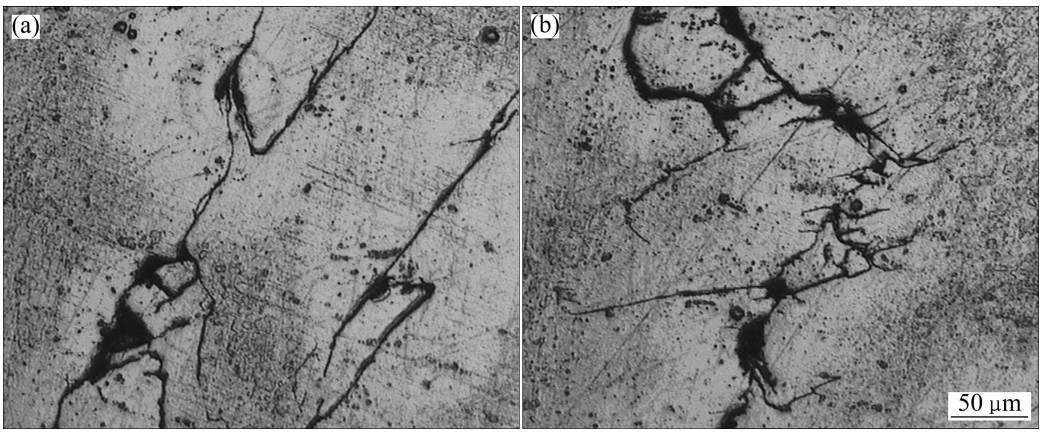

Fig. 6 Crack propagation path for AZ31B magnesium alloy: (a) Crack branching; (b) Crack propagation path

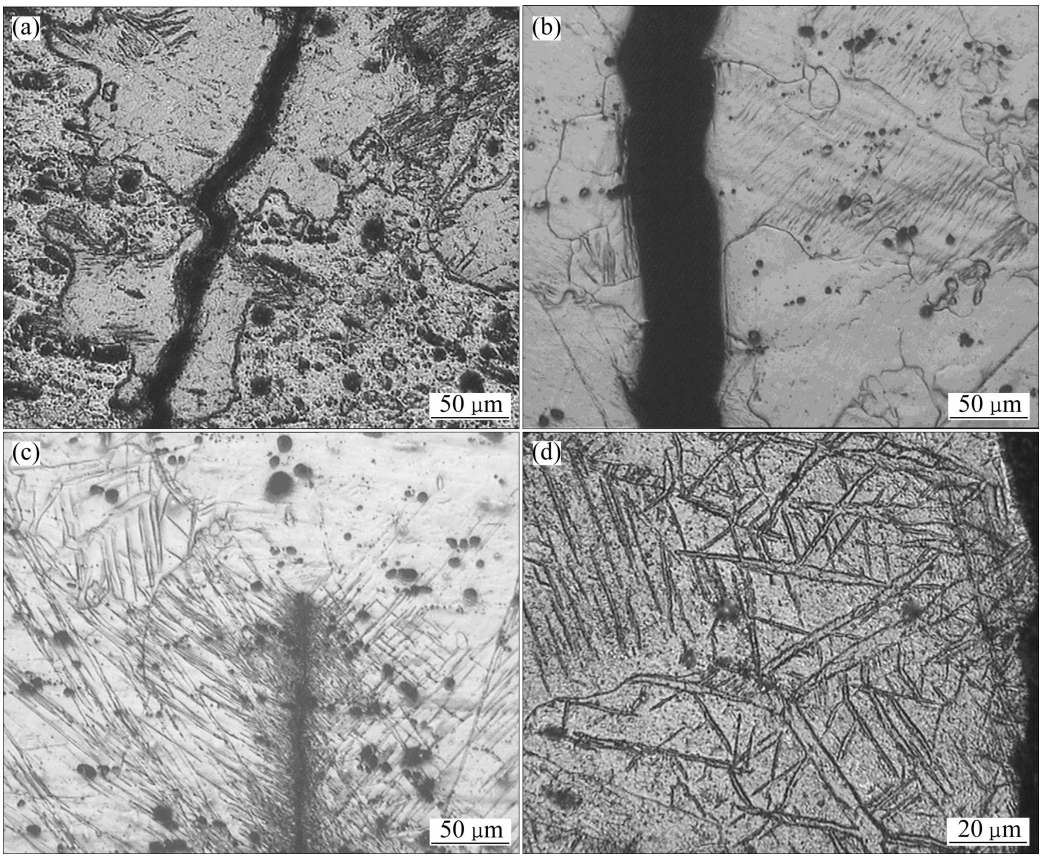

Fig. 7 Crack propagation path and twinning deformation of base metal: (a), (b) Crack propagation path; (c) Crack tip; (d) Twinning deformation near fracture

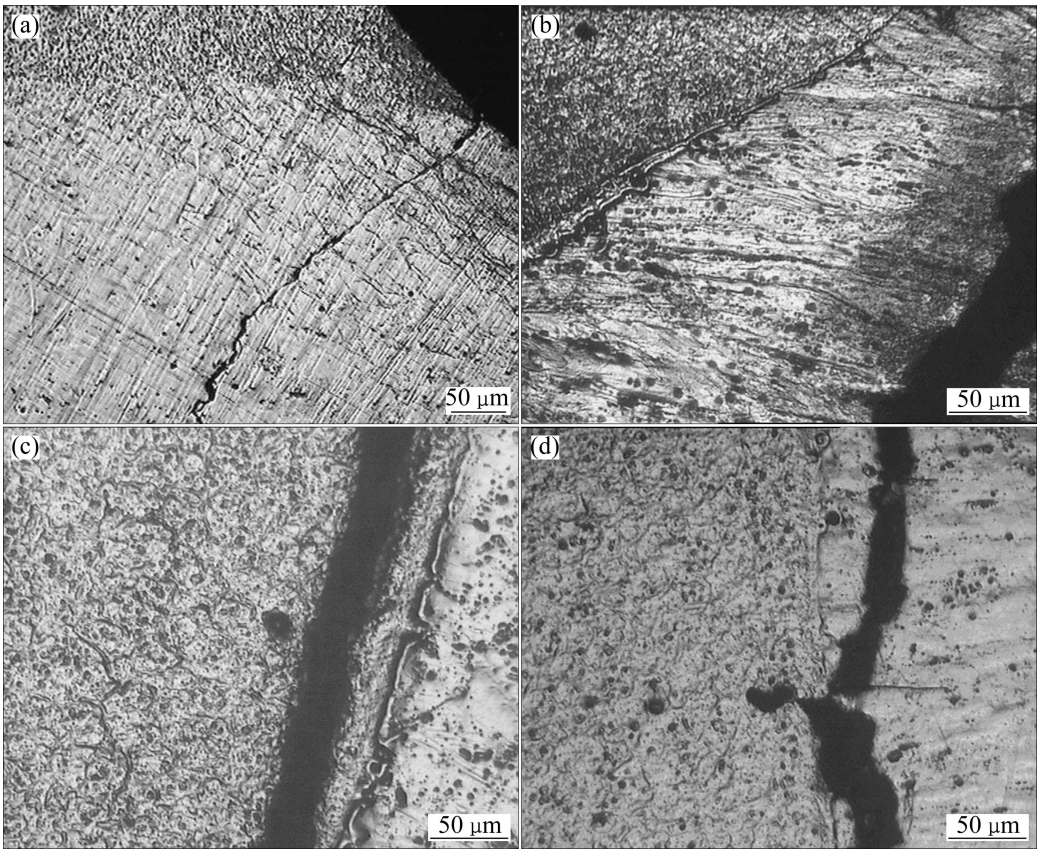

Fig. 8 Crack propagation site and path for welded joint: (a) Crack propagation site along weld toe; (b) Crack propagation along HAZ; (c), (d) Crack propagation along weld junction

3.3 Fracture analysis

Figures 9(a) and (b) show the fatigue fracture surfaces of the AZ31B magnesium alloy base metal. These images indicate that the fracture surface is characterized by quasi-cleavage and fan-shaped patterns (Fig. 9(a)). There are many tear ridges on the quasi-cleavage fracture surface, which are perforated and tipped during separate crack nucleation.

A secondary crack is observed on the fracture surface in Fig. 9(b), and its propagation direction corresponds to the rolling direction. It is observed that the slip deformation occurs on the fracture surface where cleavage steps are found, and the fracture surface is a brittle fracture. Figure 9(c) shows tensile fracture of base metal. Comparing with the fatigue fracture, the tensile fracture of base metal is quasi-cleavage fracture, and the shear lip is in the fracture.

Figure 9(d) shows the fatigue fracture surface of the butt joint. Some cleavage steps can be seen. Figure 9(e) shows the partially enlarged image of Fig. 9(d) where fatigue striation-like features are vertical to the crack propagation direction, and secondary cracks are also observed. The fatigue striation size is about 5 μm. It means that the butt joint exhibits a brittle fracture. Figure 9(f) shows the tensile fracture of the butt joint, which is characterized by dimple and is a ductile fracture.

Figure 9(g) shows the fatigue fracture surface of the transverse cross joint. Many cleavage steps can be seen. Because the fatigue crack propagates at different rates, the crack propagation has an arc path. Figure 9(h) shows partially enlarged image of Fig. 9(g), where secondary crack and cleavage step are observed.

Figure 9(i) shows that the lateral connection joint fracture surface is characterized by cleavage step. Figure 9(j) shows partially enlarged image of Fig. 9(i). The slip deformation occurs in some grain, and the lateral connection joint fails in a brittle fracture mode.

Magnesium alloy has a hexagonal close-packed structure. Its primary slip plane is a basal plane, and its slip system is less [14−15]. It only has one slip plane (0001) at room temperature and three slip directions in the slip plane (0001). Because magnesium alloy has only three geometry slip systems and two independent slip systems, whereas five slip systems are required for generalized and homogeneous plasticity [16], its plasticity is lower than the fcc and bcc metals, and its plasticity deformation relies more on twinning, as shown in Fig. 7(d). So the plasticity deformation capacity of magnesium alloy is weak. It presents a brittle fracture

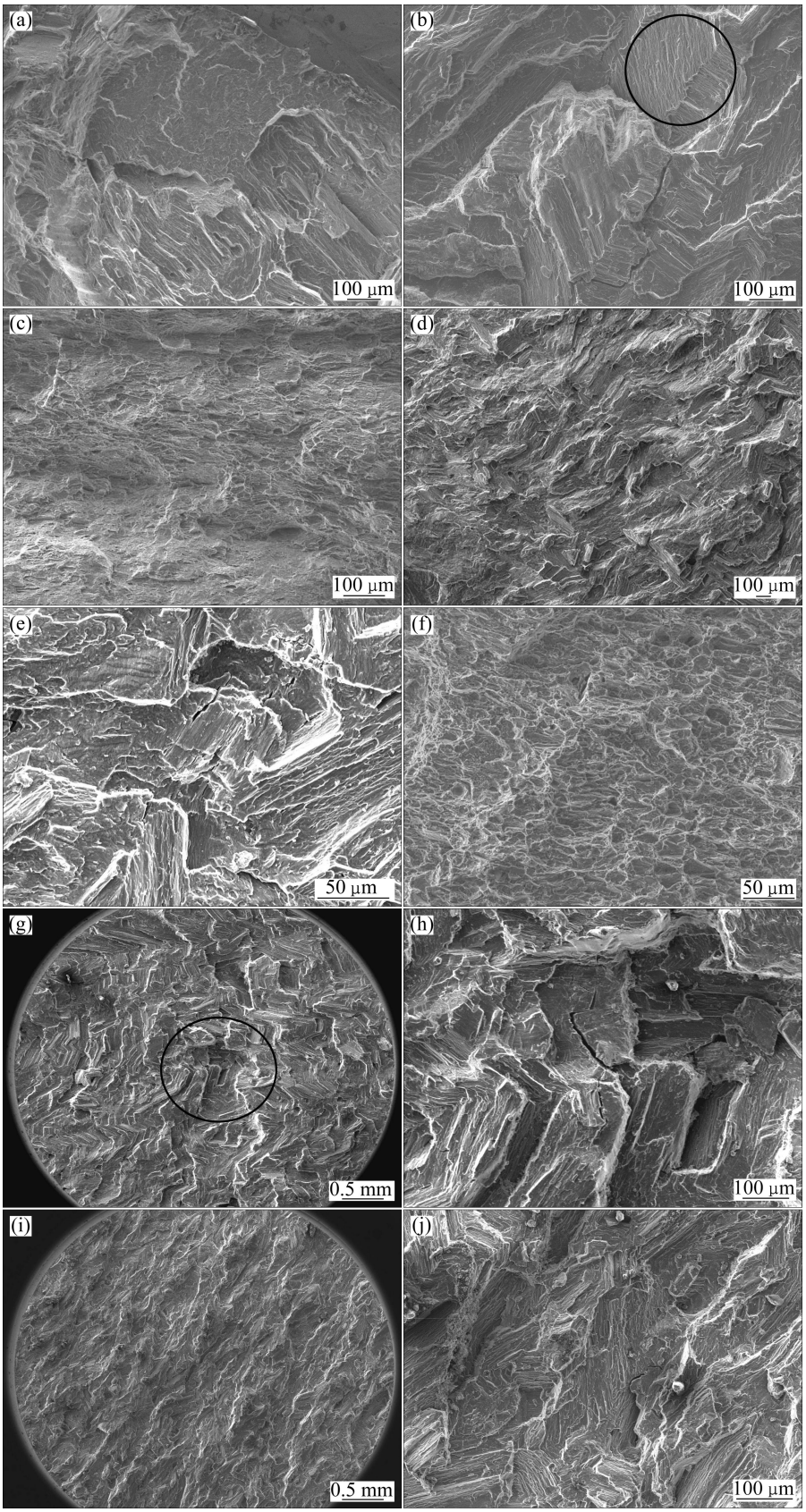

Fig. 9 Fatigue fracture appearance: (a) Tear ridge on fatigue fracture surface of base metal; (b) Secondary cracks in base metal; (c) Tensile fracture of base metal; (d) Fracture surface of butt joint; (e) Secondary cracks in butt joint; (f) Tensile fracture surface of butt joint; (g) Fracture surface of transverse cross joint; (h) Partial enlargement for Fig. 9(g); (i) Fracture surface of lateral connection joint; (j) Partial enlargement for Fig. 9(i)

characteristic while failed. The plasticity deformation capacity also depends on c/a (c is lattice height, a is side length of base plane). The c/a value of Mg is 1.623 5, slightly less than the axial ratio of 1.633 in the isometric rigid sphere model [17].

The cleavage fracture of the magnesium alloy during fatigue deformation occurs on the high index plane, and the crack shape is strongly changed because of twins and slips [17]. The fatigue fracture surface appearance is a quasi-cleavage fracture with a few secondary cracks.

In the course of crack propagation, because the grain size is nonuniform, the crack forks form, which will inhibit crack propagation. This inhibition, in turn, results in the higher fatigue strength for the magnesium alloy base metal. The stress concentration and welding residual stress occur in welded joint, and the grains in welding junction and HAZ are coarser than those in the base metal, which results in the lower fatigue strength of welded joint.

4 Conclusions

1) The fatigue strengths corresponding to a 50% survival rate of 50% for the base metal, butt joint, transverse cross joint and lateral connection joint are 66.72, 39.00, 24.38, and 24.40 MPa, respectively. The dynamic load carrying capacity of welded structure is closely related to the joint type.

2) The crack propagation macroscopic path of the AZ31B magnesium alloy base metal is smooth, while the microscopic path is twisted. Some cracks have two forks. The crack propagation is transgranular.

3) The crack initiates in the welding toe and the crack propagates along the HAZ for butt joint and transverse cross joint; the crack initiates in fillet weld leg for lateral connection joint.

4) The fatigue fracture surface consists of quasi-cleavage patterns or cleavage step and a brittle fracture occurs. There are numerous secondary cracks; some fatigue striations exist in butt joint and their size is about 5 μm.

References

[1] CHEN Zhen-hua, YAN Hong-ge, CHEN Ji-hua, QUAN Ya-jie, WANG Hui-min, CHEN Ding. Magnesium alloy[M]. Beijing: Chemical Industry Press, 2004. (in Chinese)

[2] LIU Zheng, ZHANG Kui, ZENG Xiao-qin. Theory and application of Mg matrix light alloys[M]. Beijing: China Machine Press, 2002. (in Chinese)

[3] LUO T J, YANG Y S, TONG W H, DUAN Q Q, DONG X G. Fatigue deformation characteristic of as-extruded AM30 magnesium alloy[J]. Materials and Design, 2010, 31: 1617−1621.

[4] PAN Ji-luan. Structure of magnesium alloy and welding [J]. Electric Welding Machine, 2005, 35(9): 1−7. (in Chinese)

[5] YU Kun, LI Wen-xian, WANG Ri-chu, MA Zheng-qing. Research, development and application of wrought magnesium alloys[J]. The Chinese Journal of Nonferrous Metals, 2003, 13(2): 277−288. (in Chinese)

[6] SCINTILLA L, TRICARICO D, BRANDIZZIB M, SATRIANO A A. Nd:YAG laser weldability and mechanical properties of AZ31 magnesium alloy butt joints[J]. Journal of Materials Processing Technology, 2010, 210: 2206−2214.

[7] MIAO Yu-gang, LIU Li-ming, ZHAO Jie, YU De-kai. Microstructure feature analysis of fusion welded joint of wrought Mg-alloy[J]. Transaction of the China Welding Institution, 2003, 24(2): 63−66. (in Chinese)

[8] PARK S S, TANG W N, YOU B S. Microstructure and mechanical properties of an indirect-extruded Mg-8Sn-1Al-1Zn alloy[J]. Materials Letters, 2010, 64: 31−34.

[9] ZHANG Hui, YAN Qi-qi, LI Luo-xing. Microstructures and tensile properties of AZ31 magnesium alloy by continuous extrusion forming process[J]. Materials Science and Engineering A, 2008, 486: 295−299.

[10] KARAKAS Ö, MORGENSTERN C, SONSINO C M. Fatigue design of welded joints from the wrought magnesium alloy AZ31 by the local stress concept with the fictitious notch radii of r_f=1.0 and 0.05 mm[J]. International Journal of Fatigue, 2008, 30: 2210−2219.

[11] PADMANABAN G, BALASUBRAMANIAN V. Fatigue performance of pulsed current gas tungsten arc, friction stir and laser beam welded AZ31B magnesium alloy joints [J]. Materials and Design, 2010, 31: 3724−3732.

[12] ZHANG Pei-wu, XIA Wei, LIU Ying, ZHANG Wei-wen, CHEN Wei-ping. The research of wrought magnesium alloy forming technology and its application[J]. Materials Reviews, 2005, 19(7): 82−85. (in Chinese)

[13] XU Dao-kui, LIU Lu, XU Yong-bo, HAN En-hou. Ultra-high cycle fatigue behavior of the as-extruded magnesium alloy ZK60[J]. Acta Metallurgica, 2007, 43(2): 144−148.

[14] MORDIKE BL, EBERT T. Magnesium properties applications potential[J]. Materials Science and Engineering A, 2001, 302(1): 37−45.

[15] PRASAD T V R K, RAO K. Effect of crystallographic texture on the kinetics of hot deformation of rolled Mg-3A1-1Zn alloy plate[J]. Materials Science and Engineering A, 2006, 432(1/2): 170−177.

[16] AZEEM M A, TEWARI A, MISHRA S, GOLLAPUDI S, RAMAMURTY U. Development of novel grain morphology during hot extrusion of magnesium AZ21 alloy[J]. Acta Metallurgica, 2010, 58: 1495−1502.

[17] GAO Hong-tao, WU Guo-hua, DING Wen-jiang. Review on the fatigue behavior of magnesium alloys[J]. Foundry Technology, 2003, 24(4): 266−268. (in Chinese)

AZ31B 镁合金及其焊接接头的疲劳断裂机理

张红霞，王文先，卫英慧，李晋永，王建玲

太原理工大学 材料科学与工程学院，太原 030024

摘 要：对 AZ31B 镁合金进行疲劳实验，在 2×10^6 循环次数下，母材、对接接头、横向十字接头和侧面连接接头的疲劳强度分别为 66.72，39.00，24.38 和 24.40 MPa。采用光学显微镜对裂纹扩展特征进行分析，结果表明，AZ31B 母材的疲劳裂纹宏观扩展路径平滑，但微观观察发现疲劳裂纹扩展方向曲弯，有些裂纹分成两岔；裂纹尖端扩展均为沿晶扩展。焊接接头裂纹均在焊趾部位起裂，对接接头和横线十字接头的裂纹沿着热影响区扩展；侧面连接接头的裂纹起裂位于焊脚部位。采用扫描电子显微镜对疲劳断裂机理进行分析。疲劳断口由准解理或解理台阶组成，均为脆性断裂，断口中存在二次裂纹，对接接头中存在疲劳条纹，其间距约为 5 μm。

关键词：AZ31B 镁合金；疲劳断裂；裂纹扩展；脆性断裂

(Edited by YUAN Sai-qian)